International Journal of Biological Macromolecules 255 (2024) 128354

Contents lists available at ScienceDirect

International Journal of Biological Macromolecules

journal homepage: www.elsevier.com/locate/ijbiomac

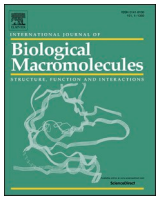

PEI functionalized cell membrane for tumor targeted and glutathione responsive gene delivery

Mengying Wang, Haoxiang Huang, Yanlin Sun, Mingjie Wang, Zhaojun Yang, Yong Shi, Liang Liu *

School of Life Science and Technology, Wuhan Polytechnic University, Wuhan 430023, China

ARTICLE INFO

Keywords:
Gene vector
Polyethylenimine
Cell membrane
Glutathione response
Tumor targeting

ABSTRACT

Polyethylenimine (PEI) is a broadly exploited cationic polymer due to its remarkable gene-loading capacity. However, the high cytotoxicity caused by its high surface charge density has been reported in many cell lines, limiting its application significantly. In this study, two different molecular weights of PEI (PEI10k and PEI25k) were crosslinked with red blood cell membranes (RBCm) *via* disulfide bonds to form PEI derivatives (RMPs) with lower charge density. Furthermore, the targeting molecule folic acid (FA) molecules were further grafted onto the polymers to obtain FA-modified PEI-RBCm copolymers (FA-RMP25k) with tumor cell targeting and glutathione response. *In vitro* experiments showed that the FA-RMP25k/DNA complex had satisfactory uptake efficiency in both HeLa and 293T cells, and did not cause significant cytotoxicity. Furthermore, the uptake and transfection efficiency of the FA-RMP25k/DNA complex was significantly higher than that of the PEI25k/DNA complex, indicating that FA grafting can increase transfection efficiency by 15 %. These results suggest that FA-RMP25k may be a promising non-viral gene vector with potential applications in gene therapy.

1. Introduction

Gene therapy has become a promising approach to treating various diseases by introducing exogenous genes into target cells to compensate for abnormal genes [1,2]. For instance, it is expected to be an effective and safe treatment for cancer, including gene immunotherapy [3], gene knockout [4,5], gene modification [6], and gene addition [7]. However, the lack of efficient and safe gene delivery technology is a major issue hindering the wide clinical application of gene therapy [8,9]. Two main gene delivery tools are currently used: viral and non-viral vectors [10–14]. Non-viral vectors, owing to their low immunogenicity, safety, and high gene loading capacity, have become increasingly popular, especially polyethyleneimine (PEI), a cationic polymer [10,15]. Despite this, challenges remain, such as the instability of the PEI/DNA complex, the potential for unexpected interactions with host biomolecules leading to cytotoxicity, capture and clearance by the immune system, and short circulation time resulting in low gene delivery efficiency [16–18].

By modifying PEI or encapsulating PEI/DNA complexes with biocompatible materials, the safety and transfection efficiency of PEI can be effectively improved [19]. After modification with molecules such as polyethylene glycol (PEG) [20], polyphenols [21], peptides [22], and amino acids [23], the cytotoxicity of PEI significantly decreased, and the transfection efficiency also improved. In addition, PEG [24], polysaccharides [25], cationic liposomes [26,27], and the complexation between organic molecules and metals [21] can also be utilized to form coatings on the surface of PEI/DNA complexes, which is known as encapsulation strategies. The encapsulation strategy can not only effectively reduce the toxicity of PEI/DNA complexes, but also improve the stability and circulation time of PEI/DNA complexes *in vivo* [28]. Liposomes are the most commonly used encapsulation materials, as they exhibit similar physicochemical properties to cell membranes, resulting in higher cell uptake efficiency in encapsulated complexes [27]. Unfortunately, however, the high charge density of cationic liposomes can also lead to significant cytotoxicity [29].

Cell membrane-coated drugs and gene delivery carriers have been widely used in various biological and biomedical research due to their excellent biocompatibility and biodegradability [30,31]. Thanks to the good fusion and biocompatibility of cell membranes, encapsulating drugs or vector/gene complexes with cell membranes can significantly improve the delivery efficiency and safety of drugs or gene vectors [32]. For example, encapsulating PEI/DNA complexes using cell membranes not only improves the transfection efficiency of the complexes, but also

* Corresponding author.
E-mail address: hustll@126.com (L. Liu).

https://doi.org/10.1016/j.ijbiomac.2023.128354
Received 4 June 2023; Received in revised form 20 November 2023; Accepted 20 November 2023
Available online 22 November 2023

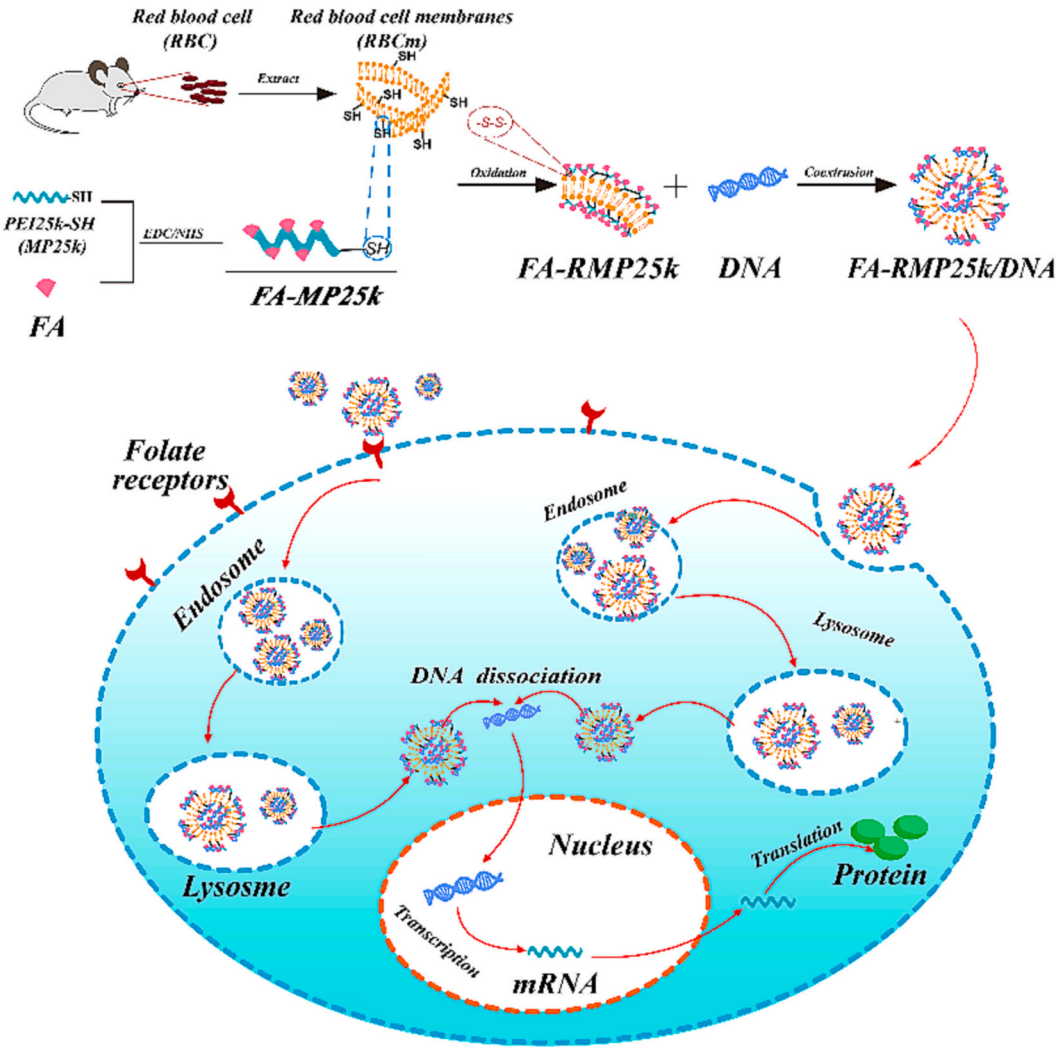

Scheme 1. Scheme for the preparation of FA-RMP25k/DNA complexes as well as the transport and gene transfection of the complexes in cells.

achieves a certain degree of cell membrane homology targeting [33]. In addition, cell membrane encapsulation strategies can also effectively improve the stability and biocompatibility of nanomaterials. The transmembrane protein CD47 of red blood cells membrane (RBCm) can interact with glycoprotein SIRPα present on phagocytes surface, and activate the tyrosine phosphatases harboring SH_2 domains, to prevent phagocytes-mediated phagocytosis and prolong the circulation time [34,35]. Therefore, the red blood cell membrane encapsulation strategy has shown unique advantages in the design of nano delivery carriers for drugs and genes.

Disulfide bonds are commonly found and stable in regular cells. But, when the environmental glutathione level is elevated, these bonds can be disrupted by exchanging thiol groups with glutathione [36,37]. Interestingly, the level of glutathione in tumor cells is reported to be four times higher than in normal cells, allowing for the specific release of disulfide-bond drugs in tumors, thereby achieving local responsiveness and targeted drug delivery [38,39]. Therefore, introducing disulfide bonds into gene delivery systems can achieve efficient gene release in tumor cells [40]. In addition, due to the fact that the folic acid (FA) receptor is a cell surface glycoprotein overexpressed on many cancer cells, FA is a high affinity ligand that targets cancer cells [41]. It has been widely used in cancer targeting therapy for 25 years and has been extensively studied in the research of breast cancer, lung cancer, and ovarian cancer [42]. A typical method is to pair FA with anticancer drugs or delivery systems, such as RNA interfering nanoparticles. After FA is recognized by receptors on the cell membrane, the nanoparticles carrying the drug can enter the cell, thereby achieving tumor-targeted delivery of the drug [43–46].

By taking inspiration from the initial work, two different molecular weights of PEI were crosslinked to biocompatible red blood cell membranes *via* disulfide bonds, resulting in the creation of PEI-RBCm (RMPs). Of these, PEI25k-RBCm (RMP25k) was chosen due to its high transfection efficiency and further modified with FA grafting (product named FA-RMP25k) to act as a tumor-targeted gene delivery vector, as shown in Scheme 1. To analyze the composition of RMP10k, RMP25k, and FA-RMP25k, Fourier transform infrared spectroscopy (FTIR) and SDS-PAGE were used. The morphology and average particle size of RMP/DNA and FA-RMP25k/DNA complexes were characterized by atomic force microscopy (AFM), transmission electron microscopy (TEM), and dynamic light scattering (DLS). The safety of FA-RMP25k was assessed using MTT and protein adsorption methods. Finally, the potential of FA-RMP25k as a gene carrier was evaluated through *in vitro* cell uptake and gene transfection experiments.

2. Materials and methods

2.1. Materials

Branched polyethyleneimine (bPEI, Mw = 10 k and 25 k Da) and folic acid (FA) was purchased from Macklin Biochemical Co., Ltd.

(Shanghai, China). Fluorescein isothiocyanate (FITC), 4′,6-diamidino-2-phenylindole (DAPI), ethidium bromide (EtBr) fluorescent dyes and 1,1′-dioctadecyl-3,3,3′,3′-tetramethylindocarbocyanine perchlorate (DiI, CM Red Fluorescent Probe) were obtained from Sigma-Aldrich (Shanghai, China). The Enhanced Green Fluorescent Protein (EGFP) plasmid was amplified in *Escherichia coli* and purified using a Maxi plasmid kit from Tiangen Biotech Co., Ltd. (Beijing, China). 3-Mercaptopropionic acid (Ma), glutathione (GSH), and dimethyl sulfoxide (DMSO) were purchased from Shanghai Macklin Biochemical Technology Co., Ltd. 3-[4,5-Dimethylthiazol-2-yl]-2,5-diphenyltetrazolium bromide (MTT) and fetal bovine serum (FBS) were obtained from China National Pharmaceutical Group Corporation (Shanghai, China). Dulbecco's modified Eagle's media (DMEM) and Active Ingredient-Active Ingredient solution (100×) were purchased from Gibco (Shanghai, China). HEK-293T, HeLa, AML- 12, HepG2 cells were obtained from the National Center for Cell Re-pository (Beijing, China) and cultured in DMEM containing 10 % FBS and 1 % Active Ingredient-Active Ingredient at 37 °C in a 5 % CO_2 humidified incubator.

2.2. Preparation

2.2.1. Synthesis of thiol PEI (MP10k and MP25k

5 mL mercaptopropionic acid (Ma) was dispersed in 15 mL dimethyl sulfoxide (DMSO), then 1.5 mL thionyl chloride ($SOCl_2$) was added dropwise to the system *via* a constant pressure funnel. After 6 h, the DMSO solution containing 200 mg PEI25k was added, and the mixture was incubated overnight for 12 h. The resulting product was placed in a 25,000 Da dialysis bag and water-dialyzed for 48 h to remove DMSO and $SOCl_2$. Finally, the collected dialysate was lyophilized to obtain thiol PEI25k (MP25k). Replacing PEI25k with PEI10k, the same method was used to prepare thiol PEI10k (MP10k).

2.2.2. Isolation of RBCm

RBCm was prepared using a hypotonic solution method. Fresh whole blood was obtained from the rat orbital venous plexus, and the upper plasma layer was carefully removed after centrifugation at 3000 rpm for 5 min at 4 °C. The resulting red blood cell precipitate was washed 2–3 times with isotonic phosphate buffered saline (PBS, pH = 7.4) until the supernatant was colorless. Afterward, cells were resuspended in pre-cooled PBS solution and subjected to hypotonic swelling treatment at 4 °C until the red blood cells were fully ruptured. The released hemoglobin was removed by centrifugation at 15,000 rpm for 5 min, leaving the lower pinkish-red cell membranes, which were then washed 2–3 times with 1 × PBS. The collected cell membrane precipitate was re-suspended in deionized water, freeze-dried, and obtained as solid RBCm fragments.

2.2.3. Preparation of PEI-RBCm graft copolymer (RMP10k, RMP25k

100 mg MP25k was added into 20 mL ethyl acetate, and sonicated for distribution. Afterward, 100 mg RBCm was added into the solution and sonicated for 15 min. After 30 min stirring, 5 mL 30 % H_2O_2 solution was added and kept stirring for another 48 h. Then the mixture was placed into a 25,000 Da dialysis bag and dialyzed in dH_2O for 72 h. The PEI25k-RBCm graft copolymer (RMP25k) was obtained by vacuum freeze-drying the dialyzed retention solution. Using MP10k instead of MP25k, PEI10k-RBCm graft copolymer (RMP10k) was prepared using the same method.

2.2.4. Preparation of FA-thiol PEI graft copolymer (FA-MP25k

50 mg FA was dissolved in 20 mL DMSO solution, then 15.5 mg 1-ethyl-(3-dimethylaminopropyl) carbodiimide hydrochloride (EDC) and 13 mg N-hydroxysuccinimide (NHS) were added. The mixture was sonicated until fully dissolved, followed by magnetic stirring for 24 h to activate the carboxylic acid groups of FA. Next, 100 mg MP25k was slowly added to the above solution in 10 mL DMSO, and stirred continuously for 3 days. The reaction mixture was placed in a 25,000 Da dialysis bag, and PBS buffer with pH 7.4 was used for dialysis to remove free FA. FA-Thiol PEI25k graft copolymer (FA-MP25k) was obtained after the retentate was collected and freeze-dried.

2.2.5. Preparation of FA modified PEI-RBCm copolymer (FA-RMP25k)

100 mg FA-MP25k was dispersed in 20 mL of ethyl acetate by sonication, followed by the addition of 100 mg of RBCm fragments to the above solution, and sonicated for 15 min, then stirred magnetically for 30 min. Subsequently, 5 mL 30 % H_2O_2 solution was added to the system and stirred magnetically for 48 h. Afterward, the mixed solution was placed in a 25,000 Da dialysis bag and water-dialyzed. The FA modified PEI RBCm copolymer (FA-RMP25k) was obtained by vacuum freeze-drying the dialyzed retention.

2.2.6. Preparation of DiI and FITC labeled FA-RMP25k (DiI-FITC-FA-RMP25k, DiI-FITC-RMP10k/RMP25k)

20 mg FA-RMP25k complex was dispersed in 10 mL deionized water, and 2 mL FITC solution (5 mg/mL) was added. The mixture was stirred under dark at room temperature (RT) for 24 h, then the above mixture was placed in a 1000 Da dialysis bag and water-dialyzed for 48 h to remove free FITC. The retentate was collected and Diluted with dH_2O to a final concentration of 1 mg/mL to obtain the FITC-labeled FA-RMP25k complex (FITC-FA-RMP25k). After FITC labeling, 20 mL FITC-FA-RMP25k complex (1 mg/mL) was mixed with 50 μL DiI solution (5 mM/mL) in a beaker and stirred in the dark at RT for 4 h. The resulting mixture was centrifuged at 15,000 rpm for 10 min at 4 °C. The precipitation was washed 3 times with dH_2O until the supernatant became colorless. Finally, The precipitation was freeze-dried and resuspended in 20 mL deionized water to obtain the DiI and FITC labeled FA-RMP25k complex (DiI-FITC-FA-RMP25k) at a concentration of 1 mg/mL. For a comparison, DiI and FITC labeled RMP10k/RMP25k (DiI-FITC-RMP10k/RMP25k) was prepared according to the same process.

2.2.7. Preparation of FA-RMP25k/DNA complex

FA-RMP25k/DNA complex was prepared by the extrusion method. FA-RMP25k and DNA was mixed well at an optimal mass ratio of 2/1 and incubated at RT for 60 min to completely bind FA-RMP25k to DNA. Then the FA-RMP25k/DNA complex was extruded 10 times across a polycarbonate membrane with a pore size of 200 nm using a Genizer liposome extruder, and stored at −20 °C after the extrusion was completed. The RMPs/DNA complex was prepared according to the same process for comparison.

2.3. Characterization

2.3.1. Sodium dodecyl sulfate-polyacrylamide gel electrophoresis (SDS-PAGE)

The effectiveness of the cell membrane coating was confirmed through SDS-PAGE electrophoresis. The gel was prepared according to the instructions of the SDS-PAGE kit (Biyuntian, Shanghai, CN). 10 μL loading buffer (5×) and a 4-fold volume of RMP or FA-RMP aqueous solution (1 mg/mL) were mixed in a boiling water bath for 10 min and centrifuged at 3000 rpm for 1 min. The supernatant was then loaded into the gel and electrophoresis was conducted at 80 V for 30 min before being increased to 120 V for 2 h until the bromophenol blue dye in the sample reached the bottom of the gel. The gel was then stained with G250 for 1 h and completely decolorized with a decolorization solution, and finally imaged using a gel imaging system (Gel Doc XR, Bio-RadUS).

2.3.2. FTIR

FTIR was used to determine whether the FA-RMP25k complex was successfully synthesized by measuring the surface groups of the samples. Specifically, 1 mg FA-RMP25k complex was mixed with 100 mg of potassium bromide (KBr) powder and ground until the particle size was smaller than 2 μm. The resulting mixture was then pressed into a transparent sheet using an oil press at a pressure of 5–10 × 10^7 Pa, and

its absorption was measured at 500–4000 cm^{-1} using a FTIR spectrophotometer (INVENIO, BRUKER, GER). Using the same method, the FTIR spectra of FA, MP10k, MP25k, MA, PEI10k, and PEI25k were measured for comparison.

2.3.3. Determination of sulfhydryl content

5′,5′-Dithiobis (2-nitrobenzoic acid) (DTNB) reacts with sulfhydryl groups and produces detectable products in proportion, so it can be used to accurately measure the number of sulfhydryl groups before and after the cell membrane modification. 20 μL RBCm (1 mg/mL), RMP10k (1 mg/mL), and RMP25k (1 mg/mL) were separately added to 100 μL DTNB solution (1 mg/mL), Diluted with dH_2O to a final volume of 1 mL, and mixed by vortexing. The mixture was allowed to stand for 5 min, and the absorbance was measured at 412 nm wavelength by a multifunctional microplate reader (EnSpire™, PerkinElmer US). The absorbance of the glutathione standard was measured using the same method to fit a standard curve. The sulfhydryl content of the sample was calculated by formula (1). where C_1 is the concentration obtained from the standard curve for the sample reacted with DTNB, and C_0 is the final concentration of the sample in DTNB.

$$\text{Sulfhydryl content} = \frac{c_1}{c_0 \times 307.32} \tag{1}$$

2.3.4. Determination of primary amine content

To determine the content of primary amines, 50 μL PEI10k solution (1 mg/mL) was added to 100 μL fluorescamine solution (1 mg/mL), mixed by vortexing, and then reacted at 50 °C for 30 min. The mixture was scanned using 3D fluorescence spectroscopy with an excitation wavelength range of 320–410 nm and an emission wavelength range of 450–600 nm to determine the maximum excitation and emission wavelengths. The fluorescence intensity was measured at an excitation wavelength of 390 nm and emission wavelength of 490 nm, and a standard curve was fitted. The content of primary amines in the sample was calculated according to formula (2), where c_1 is the concentration obtained from the standard curve for the sample reacted with fluorescamine, and c_0 is the final concentration of the sample in the fluorescamine mixture.

$$\text{Primary amine content} = \frac{c_1 \times 8.2 \times 10^{-6}}{c_0} \tag{2}$$

2.3.5. Particles size and zeta potential

RMPs/DNA and FA-RMP25k/DNA complexes were prepared according to Section 2.2.7, and their particle size and Zeta potential were measured using a Zetasizer Nano ZS (Malvern, U.K.) at 25 °C. The RMP10k/DNA mass ratios were 1/1, 2/1, 3/1, and 4/1, and the RMP25k/DNA mass ratios were 0.5/1, 1/1, 1.5/1, and 2/1. The FA-RMP25k/DNA mass ratio was 2/1.

2.3.6. AFM and TEM

The morphology of FA-RMP25k/DNA, RMPs/DNA complexes was observed using AFM and TEM. The complexes were prepared according to Section 2.2.7 and diluted with dH_2O, after which 50 μL of the complex solution was dropwise to the treated mica sheets, dried at RT and observed by AFM (MultiMode8I, Bruker, GER) in tapping-mode. The AFM height profiles were analyzed and quantified using Gwyddion (Version 2.58) software. Meanwhile, the complex solution was dropwise onto a copper mesh and observed by a TEM (HT7800, HITACHI, JPN) at 120 kV after drying at RT.

2.4. Bovine serum albumin (BSA) adsorption

The protein adsorption capacity was determined using a spectroscopic method, and a standard curve was generated based on the absorbance of a BSA standard solution after reaction with G250 solution. To measure the adsorption rate, 1 mL of RMPs solution (1 mg/mL) was added to 1 mL of BSA solution (1 mg/mL), incubated at 37 °C for 30 min and then centrifuged at 10,000 rpm for 10 min. Afterwards, 30 μL of the supernatant was mixed with 1 mL of G250 solution and left for 5 min. The absorbance was measured at a wavelength of 595 nm, and the concentration of BSA was calculated from the standard curve. The protein adsorption rate was determined using formula (3), where m_0 is the mass of BSA added to the carrier and m is the mass of BSA in the supernatant.

$$\text{Adsorption rate}\ (\%) = \frac{m_0 - m}{m_0} \times 100\% \tag{3}$$

2.5. DNA encapsulation and release

To investigate the effect of mass ratio on the DNA encapsulation efficiency of complexes, vector/DNA complexes were created following the method in Section 2.2.7 with the mass ratios of RMP10k/DNA, RMP25k/DNA, and FA-RMP25k/DNA set at 1/1–4/1, 0.5/1–2/1 and 0.5/1–1 respectively, and the total amount of DNA kept at 0.4 μg. The supernatant was centrifuged at 10,000 rpm for 10 min, and the DNA concentration in the supernatant was determined by aspirating the supernatant and calculating the encapsulation rate of DNA based on formula (4), where c_0 is the initial DNA concentration before complexes preparation and c is the DNA concentration in the supernatant. In addition, the effect of preparation time on the DNA encapsulation efficiency of the complex was investigated using the same method.

To analyze the release rate of the complex *in vitro*, RMP10k/DNA (4/1), RMP25k/DNA (mass ratio = 2/1), FA-RMP25k/DNA (mass ratio = 2/1), PEI10k/DNA (mass ratio = 2.5/1) and PEI25k/DNA (mass ratio = 0.75/1) were prepared according to section 2.2.7. The complexes were centrifuged at 10,000 rpm to separate out free DNA, then dispersed in 5 mL PBS. The experimental and control groups were set up with 2 mM GSH in the experimental group and not in the control group, and placed in a shaker at 37 °C and 100 rpm shaking. At predetermined time points, 100 μL of the solution was centrifuged at 10,000 rpm for 1 min, and the concentration of free DNA in the supernatant was determined. To the system, 100 μL of PBS buffer was added, and the DNA release rate was calculated using formula (5), where m_0 is the mass of DNA bound to the vector and m is the mass of DNA in the buffer.

$$\text{Encapsulation efficiency}(\%) = \frac{c_0 - c}{c_0} \times 100\% \tag{4}$$

$$\text{Release rate}\ (\%) = \frac{m}{m_0} \times 100\% \tag{5}$$

In order to more visually observe and analyze the responsive release process of FA-RMP25k/DNA complex in GSH environment, DiI-FITC-FA-RMP25k/DNA (mass ratio = 2/1) were prepared according to the above. DiI-FITC-FA-RMP25k/DNA complexes from experimental and control groups were placed in a complete medium environment at 37 °C, 100 rpm for 6 h. After that, 10 μL of the samples were taken on slides to achieve fluorescence imaging under a fluorescence confocal microscope, respectively.

2.6. Agarose gel retention assay

The DNA binding ability and protection effect of the obtained polymers were evaluated by an agarose gel retardation assay. For DNA condensation ability, RMP10k/DNA, RMP25k/DNA, and FA-RMP25k/DNA with various mass ratios were prepared according to Section 2.2.7, then loaded into a 1 % agarose gel containing EtBr, and electrophoresed for 40 min at 120 V. Afterwards, the gel was observed and analyzed by a gel imaging system (GeldocEZ, Bio-Rad, USA). To evaluate DNA protection ability, FA-RMP25k/DNA, RMP10k/DNA, RMP25k/DNA, PEI10K/DNA and PEI25K/DNA complexes were prepared with mass ratio of 2/1, 4/1, 2/1, 2.5/1 and 0.75/1 respectively, following the method in Section 2.2.7. Group I served as the control,

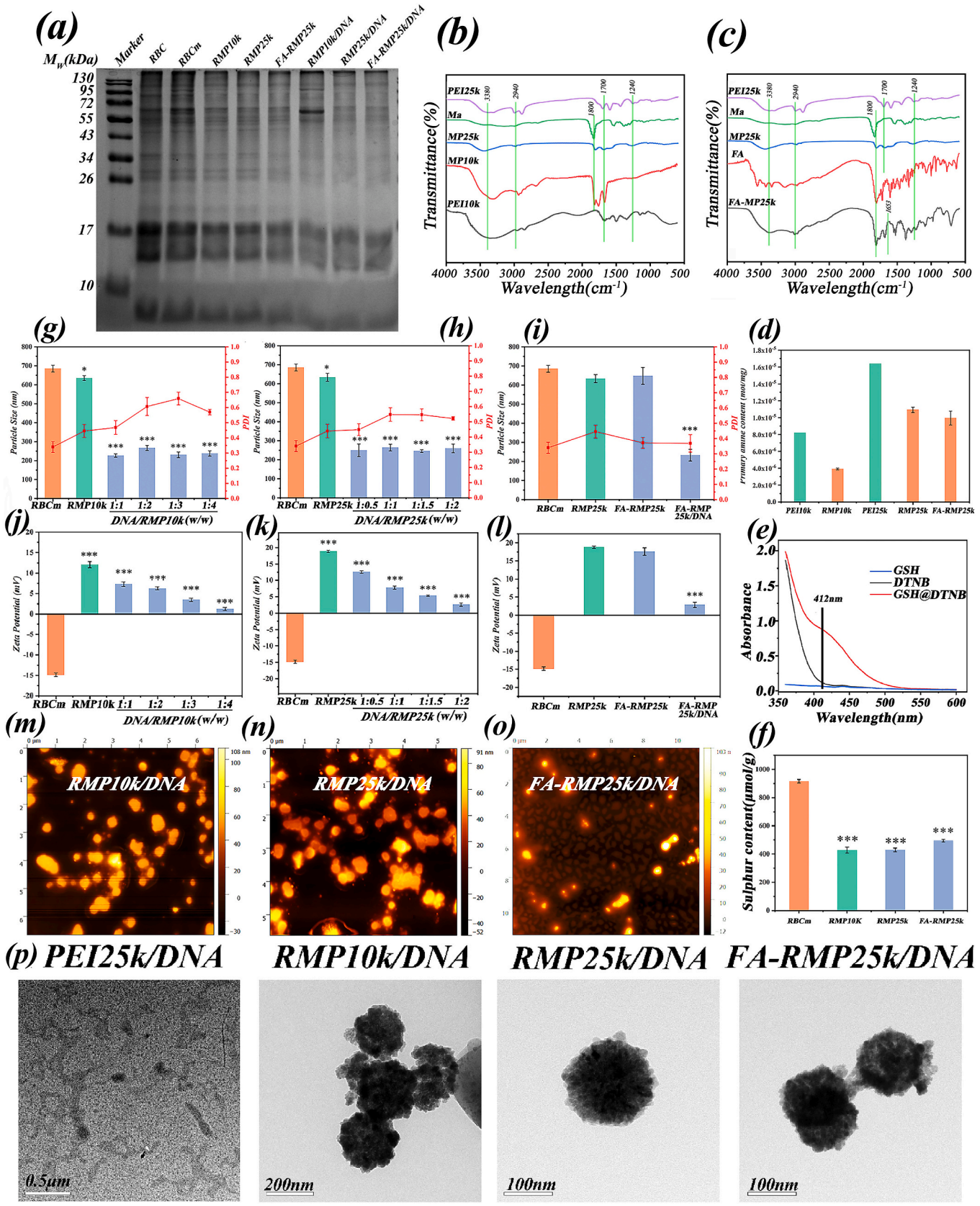

Fig. 1. Characterization results of RMPs and FA-RMP25k. (a) SDS-PAGE electrophoresis result of RMPs and FA-RMP25k. (b–c) Infrared spectra of MPs and FA-MP25k. (d) Primary amino content of RMPs, and FA-RMP25k. (e) UV–Vis absorption spectra of DTNB, GSH, GSH@DTNB. (f) Sulfhydryl content of RMPs, FA-RMP25k. (g–i) Particle size results. (j–l) Zeta potential results. (m–o) AFM results. (p) TEM results. (The experimental group was compared with the RBCm group, mean ± SD, n = 3, $*p \leq 0.05$, $***p \leq 0.0005$).

with no treatment. In Group II, a combination of 2.5 μL of 40 U/mL DNase I and 2.5 μL of 10× Reaction Buffer was mixed together and incubated at 37 °C for 2 h. Group III had 8 μL of 20 mg/mL Active Ingredient sodium solution added and incubated at 37 °C for 2 h. Group IV was first treated with 2.5 μL of 40 U/mL DNase I and 2.5 μL of 10× Reaction Buffer in a water bath at 37 °C for 2 h, then 2 μL 5 mM/L ethylene diamine tetraacetic acid (EDTA) was added in a water bath at 65 °C for 10 min to deactivate DNase I, and finally 8 μL of 20 mg/mL sodium Active Ingredient solution was added and incubated at 37 °C for 2 h. Group V was first incubated with 8 μL of 20 mg/mL sodium Active Ingredient solution for 2 h at 37 °C, followed by the addition of 2.5 μL of 40 U/mL DNase I and 2.5 μL of 10× Reaction Buffer for 2 h in a water bath at 37 °C. Subsequently, all samples underwent electrophoresis using the same conditions.

2.7. Cytotoxicity

The MTT assay was used to evaluate the cytotoxicity of RMP10k, RMP25k, FA-RMP25k and other polymers on HEK 293T, HeLa, AML-12 and HepG2 cells. Cells were seeded in 96-well plates at a density of 1×10^4 cells per well and incubated for 24 h. Afterward, the vector/DNA complex was added to the cells with new medium and incubated for 48 h. Following this, the cells were washed three times with PBS and MTT (0.5 mg/mL) was added. After a further 4 h of incubation, the MTT solution was removed and DMSO was added to each well to dissolve the blue-purple methylzan crystals. Subsequently, the absorbance of each sample at 570 nm was measured using a multifunctional microplate reader. Cell viability was calculated based on formula (6), where A_0 was the absorbance at 570 nm of the cells treated with the complete medium, A_b was the absorbance at 570 nm of blank wells containing complete medium and MTT solution without cells and A was the absorbance at 570 nm of the cells treated with the various Control/DNA complexes.

$$\text{Cell viability (\%)} = \frac{A - A_b}{A_0 - A_b} \times 100\% \quad (6)$$

2.8. In vitro uptake efficiency evaluation

The cellular uptake efficiency of RMP10k/DNA, RMP25k/DNA and FA-RMP25k/DNA complexes was investigated in 293T cells and HeLa cells. To facilitate observation, DiI and FITC labeled RMP10k, RMP25k and FA-RMP25k were prepared according to the method described in Section 2.2.6, while RMP10k/DNA, RMP25k/DNA and FA-RMP25k/DNA complexes were prepared according to the method in Section 2.2.7. After the cell density reached 80–90 %, the culture medium was replaced with a DMEM dispersion of the complex and the cells were incubated for 6 h. After removing the complex DMEM dispersion, the cells were washed three times with PBS and fixed with paraformaldehyde. Following staining with DAPI, the uptake of the complex in the cells was observed using inverted fluorescence microscopy (BA400, Motic, China) and confocal laser scanning microscopy (Stellaris 6, Leica, GER). Additionally, flow cytometry (CytoFLEX, BECKMAN, US) was used to quantify the cellular uptake efficiency of complexes. For comparison, the cellular uptake efficiency of PEI/DNA complexes was also examined.

2.9. In vitro gene transfection

Mixed EGFP plasmids with RMPs and FA-RMP25k according to Section 2.2.7 to prepare RMP10k/DNA, RMP25k/DNA and FA-RMP25k/DNA complexes. After inoculating cells into a 24 wells plate with a density of 80 %, the complete culture medium was replaced with DMEM dispersion of the complexes. After 6 h of cultivation, the complexes were removed and the cells were cultivated in antibiotics free medium for 48 h. The transfection efficiency of the complexes in 293T cells and HeLa cells was observed and analyzed using an inverted fluorescence microscope, confocal laser scanning microscope (CLSM) and flow cytometry (FCM).

2.10. Statistics analysis

Statistical analysis was performed using GraphPad Prism software. Data were analyzed using Student test and one-way analysis of variance (ANOVA). $p < 0.05$ was considered statistically significant.

3. Results and discussion

3.1. Characterization

3.1.1. SDS-PAGE

After the preparation of RMPs, FA-RMP25k and FA-RMP25k/DNA complexes, the feasibility of the preparation scheme was verified and the physicochemical properties of these complexes were characterized through various methods. Firstly, SDS-PAGE electrophoresis was used to verify the retention of cell membrane proteins in RMPs and FA-RMP25k complexes. As shown in Fig. 1a, although some membrane proteins were lost during the extraction process, resulting in lower protein content in the complex compared to the intact cell membrane, the cell membrane fragments in RMP10k, RMP25k and FA-RMP25k retained the majority of red blood cell membrane proteins. RMPs, FA-RMP25k, and RBCm exhibit similar protein bands, indicating that the sample was successfully prepared and most of the membrane proteins were retained in RMPs and FA-RMP25k. Overall, in the preparation process of RMPs, FA-RMP25k, and their complexes with DNA, most membrane proteins are retained, which can endow the vector/DNA complex with biomimetic properties similar to red blood cells *in vivo*, and may be beneficial for improving their safety and transfection efficiency.

3.1.2. FTIR

The FTIR spectrum of MP10k, MP25k, FA-MP25k, FA, PEI, and Ma were illustrated in Fig. 1b–c. As observed, the appearance of the amino characteristic peak of PEI and the carbonyl characteristic peak of Ma in MP10k and MP25k demonstrated that the strategy of grafting PEI10k and PEI25k on Ma was successfully achieved. Compared to FA, FA-MP25k showed new peaks at 3380 cm^{-1} (N—H) and 2940 cm^{-1} (-CH), which demonstrated the successful synthesis of FA-MP25k. It can be seen that in the IR spectra of PEI25k and PEI10k at 3380 cm^{-1} is the stretching resonance peak caused by the amino group, 2940 cm^{-1} and 2840 cm^{-1} is the stretching resonance peak induced by -CH, 1700 cm^{-1} and 1570 cm^{-1} are the stretching vibration peak attributed to N—H of primary and secondary amines, and 1240 cm^{-1} is the stretching vibration peak caused by C—N bond [47]. In the IR spectrum of mercaptopropionic acid (Ma), the stretching resonance peak of the carbonyl group (-COOH) is at 1800 cm^{-1}. Compared with Ma, MP10k, and MP25k obtained after the condensation reaction showed stretching vibration peaks at 3380 cm^{-1} (N—H), 2940 cm^{-1} (-CH), 1700 cm^{-1} (N—H), 1240 cm^{-1} (C—N) and 1800 cm^{-1} (-COOH) out, which proved that PEI10k and PEI25k were successfully grafted on Ma. In the IR spectrum of FA, the stretching resonance peak of the carbonyl group (-COOH) at 1800 cm^{-1}, and the stretching resonance peak of the benzene ring skeleton in the region of 1400 cm^{-1}– 1600 cm^{-1} [48]. Compared with FA, FA-MP25k showed new peaks at 3380 cm^{-1} (N—H) and 2940 cm^{-1} (-CH), which demonstrated the successful synthesis of FA-MP25k. In addition, a wider absorption band is formed at 1653 cm^{-1}, which belongs to the stretching vibration of C═O in the amide [49]. It also proves that the reaction between FA and PEI is successful.

3.1.3. Determination of amino group content

The amino group content in polymer RMPs and FA-RMP25k complex was addressed, as shown in Fig. S1a and b, PEI10k exhibited the expected excitation and absorption wavelength, as well as linear correlation between its concentration and the maximum absorbance. Compared to PEI10k (8.2×10^{-6} mol/mg), PEI25k (1.64×10^{-5} mol/mg) has

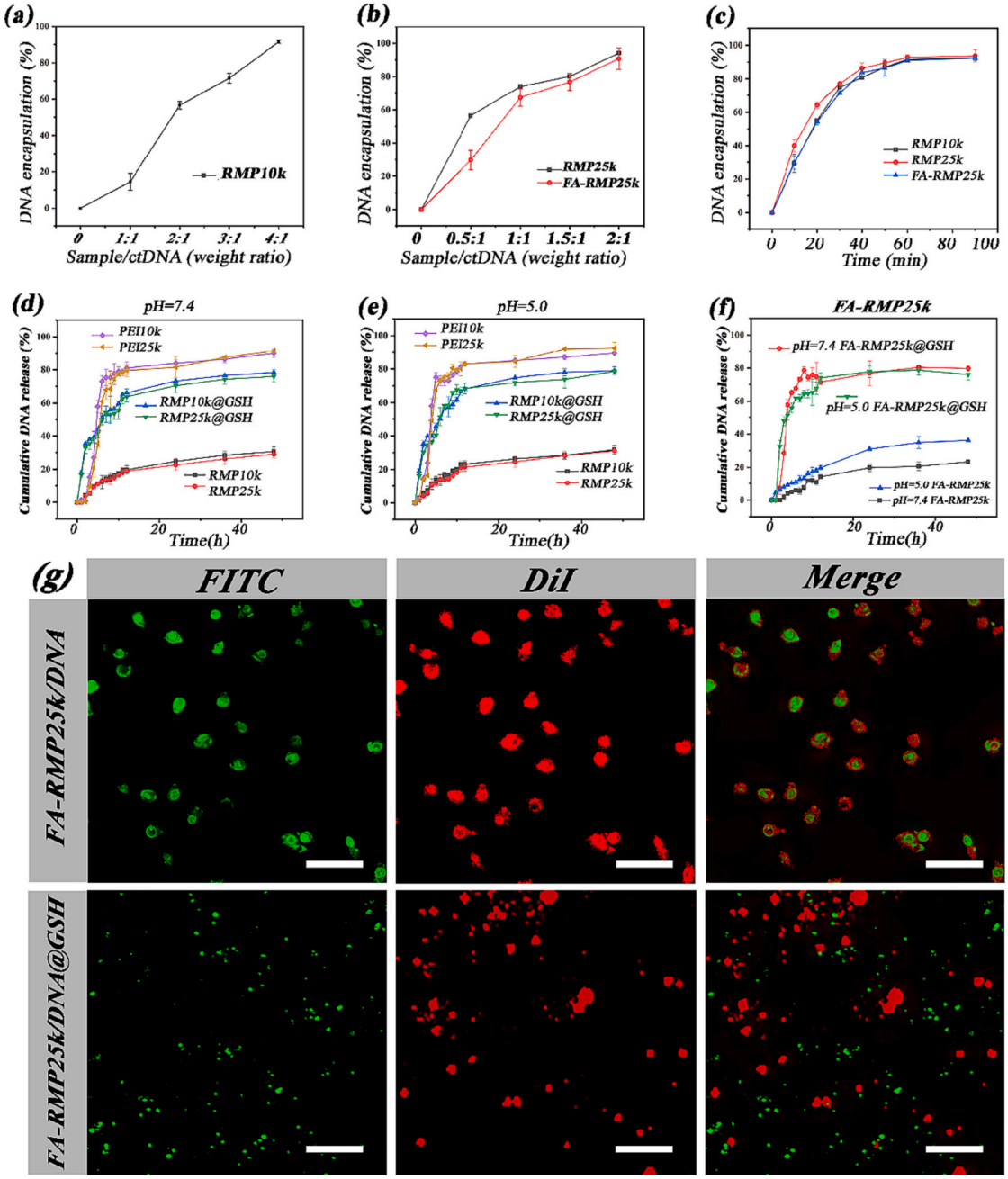

Fig. 2. The encapsulation efficiency of RMPs and FA-RMP25k complexes for DNA at different concentrations (a–b) and reaction times (c). (d–e) DNA release efficiency of RMPs/DNA complexes and (f) FA-RMP25k/DNA complexes before and after the addition of GSH at pH = 7.4 and pH = 5.0, with PEI10k and PEI25k as control groups. (g) Fluorescence images (400×) of FA-RMP25k/DNA complexes before and after the addition of GSH at complete medium (scale bar = 1 μm).

around two times more amine content, the similar difference was observed between RMP10k (3.90×10^{-6} mol/mg) and RMP25k (1.09×10^{-5} mol/mg) in Fig. 1d. In conclusion, the data suggests the higher the molecular weight of the PEI molecular, the more primary amine content of the resulted RMPs complex. Interestingly, the amino content of FA-RMP25k (9.83×10^{-6} mol/mg) was slightly reduced than that of RMP25k, indicating that FA grafting may consume part of the amino group.

3.1.4. Determination of sulfhydryl content

As shown in Fig. 1e, the sulfhydryl group in GSH reacted with DTNB and appeared a new absorption peak at 412 nm, and a good linear relationship between the absorbance of GSH standard solution at 412 nm and the concentration of GSH solution could be observed according to Fig. S1c. As shown in Fig. 1f, the surface sulfhydryl content of RBCm was 922.23 μmol/g, and the surface sulfhydryl content of the products generated after the reaction with MPs was 425.83 μmol/g for RMP10k and 418.9 μmol/g for RMP25k. The grafting rates of disulfide bonds for RMP10k and RMP25k were calculated by Eq. (1) as 46.17 % and 45.42 %, respectively. The experimental results show that the surface of RBCm is very abundant in sulfhydryl groups, which can be used as binding sites for biochemical reactions.

3.1.5. Particle size and zeta potential

Since the Zeta potential and particle size are important properties of the non-viral gene delivery vectors, both properties were measured. As reported in Fig. 1g–i, the sizes of RBCm and RMPs are 700 nm and 650 nm, respectively, implying the reactions with MPs did not alter the

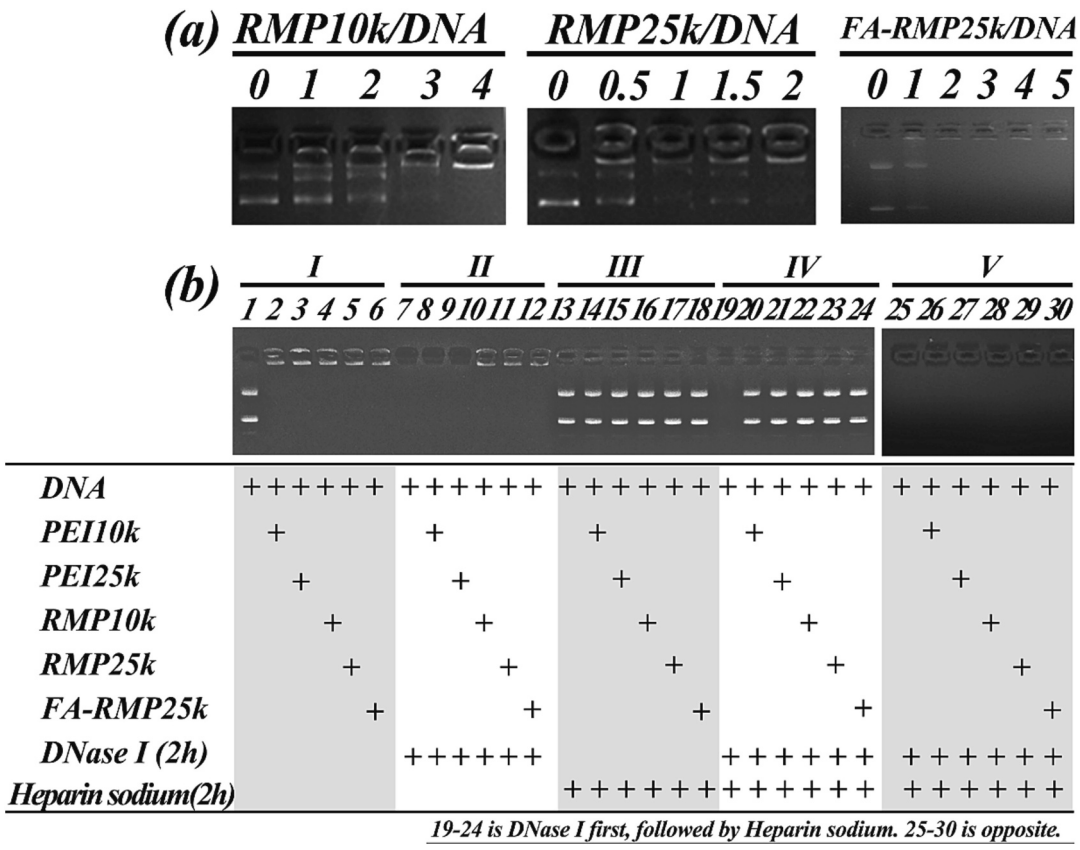

Fig. 3. DNA condensation and protection results. (a) Gel electrophoresis results of RMP10k, RMP25k, and FA-RMP25k complexes with DNA at different mass ratios. (b) Gel electrophoresis results in DNA protection and release ability of complexes formed by PEI10k, PEI25k, RMP10k, RMP25k and FA-RMP25k.

particle size. Interestingly, the particle size of FA-RMP25k/DNA complex obtained after FA-RMP25k and DNA extrusion by Genizer liposome extruder is <300 nm. After the same treatment of RMP10k and RMP25k, the particle size of both RMP10k/DNA, RMP25k/DNA complexes decreased to between 200 nm and 300 nm, and their polydispersity coefficients were in the range of 0.3–0.6, which indicated that the complexes had good dispersibility.

Since the Zeta potential was related to cytotoxicity and a high surface charge usually caused cytotoxicity, the Zeta potential of the various vector/DNA complexes was investigated. The lower positive charge density can not only ensure that the carrier/DNA complex fuses with the cell membrane and then is absorbed by the cells, but also is conducive to the safety of the complex. As shown in Fig. 1j–l, the zeta potential of the complex gradually decreases with the increase of the proportion of DNA in the carrier/DNA complex, because the positive charge densities of RMP10k, RMP25k, and FA-RMP25k are reduced after binding with the negatively charged DNA. As illustrated in Fig. 1j–k, when a constant amount of RMP complex was combined with different doses of DNA, the potential of the RMP10k/DNA and RMP25k/DNA complex decreased gradually to 1.20 mV and 2.60 mV respectively. The potential of the FA-RMP25k/DNA complex (Fig. 1l) is significantly lower than that of FA-RMP25k, which is also due to the weakening of the positive charge of the polymer by the negative charge of DNA.

3.1.6. AFM and TEM

As seen in Fig. 1m–p, the RMP10k/DNA, RMP25k/DNA and FA-RMP25k/DNA complexes have spherical or ellipsoidal particles between 200 and 300 nm, which is in line with the DLS particle size [50]. However, some particles aggregates were also observed, and this should be further addressed to avoid aggregates formation. The TEM results (Fig. 1p) showed more detailed morphological characteristics of the RMPs/DNA and FA-RMP25k/DNA complex. RMPs hybridizes with DNA during the extrusion process, forming a spherical nanocomposite with a particle size of approximately 200 nm, rather than the core-shell structural characteristics exhibited by the nanoparticles encapsulated in the unmodified cell membrane. As can be seen from the TEM result of FA-RMP25k/DNA and RMPs/DNA complexes, there is no obvious difference in the morphology of the complexes, which may be due to the same preparation method. In addition, PEI/DNA complexes exhibit irregular morphological features [51].

3.2. BSA adsorption

The ideal nano-particles used for gene delivery should have a low binding affinity with nonspecific proteins during circulation, therefore avoiding thrombosis or allergic reactions. As indicated in Fig. S1d–e the maximum absorption wavelength was 595 nm after reacting BSA with G250, and a good linear relationship was shown between the concentration of the BSA standard series and its absorbance at 595 nm. As revealed in Fig. S1f, the binding rate of RMP10k, RMP25k and FA-RMP25k with BSA is 21.28 %, 31.53 % and 29.83 %, respectively, which is lower than that of PEI10k and PEI25k, suggesting that the yielded polymers have good biosafety, and can be further investigated as a potential gene delivery vector.

3.3. DNA encapsulation and release

The efficiency of DNA encapsulation is crucial for gene delivery vectors as it determines their gene carrying capacity. As shown in Fig. 2a–b, the encapsulation efficiency of RMP10k, RMP25k, and FA-RMP25k on DNA is directly proportional to the mass ratio of vector/DNA complexes. RMP10k/DNA, RMP25k/DNA, and FA-RMP25k/DNA exhibit the highest DNA encapsulation efficiency at mass ratios of 4/1, 2/1, and 2/1, respectively, with values of 91.43 %, 94.09 %, and 90.76

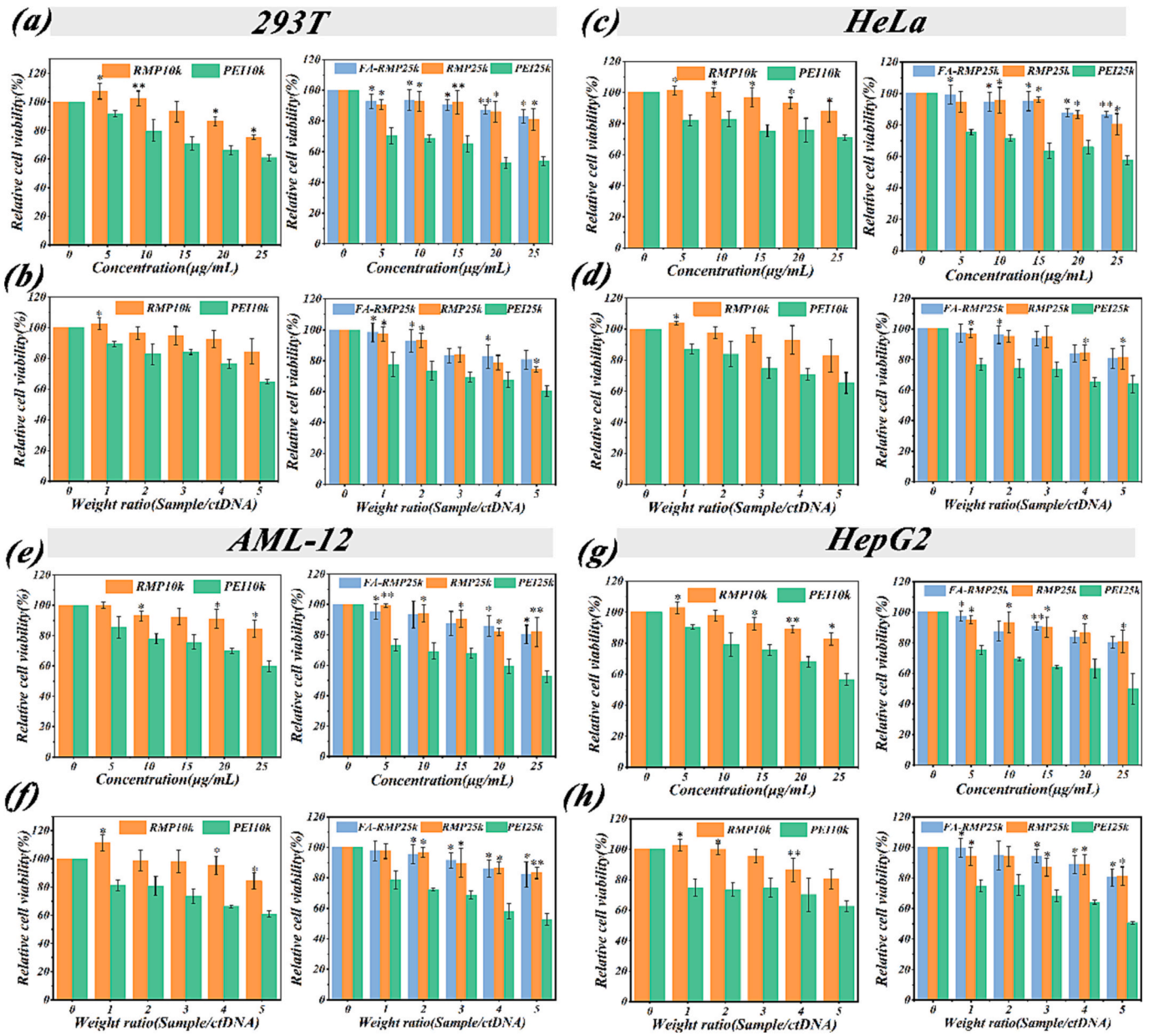

Fig. 4. MTT assay results. Relative cell viability of 293T cells (a), HeLa cells (c), AML-12 cells (e) and HepG2 cells (g) that were treated with PEI10k, PEI25k, RMP10k, RMP25k and FA-RMP25k. Relative cell viability of 293T cells (b), HeLa cells (d), AML-12 cells (f) and HepG2 cells (h) that were treated with PEI10k/DNA, PEI25k/DNA, RMP10k/DNA, RMP25k/DNA and FA-RMP25k/DNA complexes. (The experimental group was compared with the PEI group, mean ± SD, n = 3; $*p \leq 0.05$, $**p \leq 0.01$).

%, respectively. As shown in Fig. 2c, the vectors and DNA with the above mass ratios showed the highest DNA encapsulation efficiency after 60 min of incubation, which were 91.58 %, 92.90 %, and 90.90 %, respectively. The DNA release efficiency in the physiological environment and tumor microenvironment is shown in Fig. 2d–f. In a normal physiological simulation environment, the release rates of RMPs/DNA and FA-RMP25k/DNA are slower than those of PEI. In the presence of GSH, the DNA release rate and efficiency are significantly increase. This is because the disulfide bond in the complex is disrupted by glutathione, leading to rapid and massive release of DNA. In addition, as shown in Fig. 2g, the FA-RMP25k/DNA complexes in buffer environment showed a regular globular structure, which was similar to the globular structure presented in the TEM image. Interestingly, the complexes in the GSH environment showed a very distinct separation of fluorescent spots, which in combination with the results of the DNA release rate of the complexes suggests that the FA-RMP25k/DNA complexes can achieve responsive release of DNA through disulfide bond breaking. Considering the overexpression of GSH in tumor cells, these results indicate that it is feasible to use PEI to functionalize cell membranes through disulfide bonds to prepare DNA delivery systems with tumor microenvironment response.

3.4. DNA protection ability

Firstly, the DNA condensation ability of RMPs and FA-RMP25k was investigated by gel electrophoresis. As shown in Fig. 3a, with the increase of the mass ratio of RMPs/DNA and FA-RMP25k/DNA, the DNA bands in the gel gradually disappear, which means that the DNA is completely condensed, so it is blocked in the sample well, indicating that RMP and FA-RMP have the ability of DNA condensation.

As shown in Fig. 3b, lanes 1–6 show the electrophoresis results of naked DNA, PEI10k/DNA, PEI25k/DNA, RMP10k/DNA, RMP25k/DNA

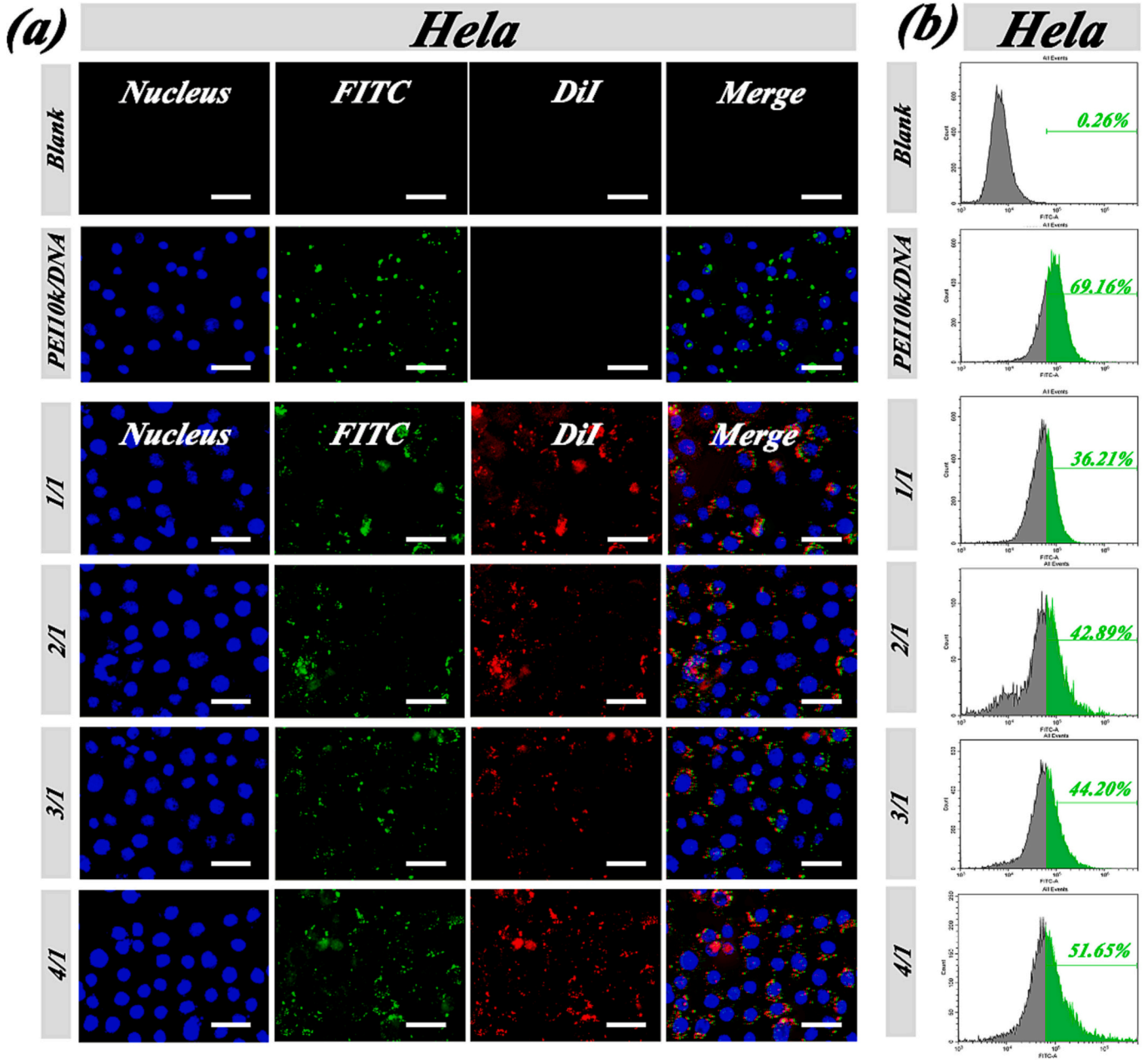

Fig. 5. Cell uptake results of RMP10k/DNA complexes in HeLa cells. (a) Fluorescence images (400×) of HeLa cells treated by DiI-FITC-RMP10k/DNA complexes (scale bar = 50 μm). (b) FCM results of the uptake efficiency of DiI-FITC-RMP10k/DNA complexes.

and FA-RMP25k/DNA complexes. The gel image shows that DNA in 2–6 lanes is completely blocked in the sample well except bare DNA which shows clear electrophoresis bands. In group II, lanes 7–12 show the electrophoresis results of DNA, PEI10k/DNA, PEI25k/DNA, RMP10k/DNA, RMP25k/DNA and FA-RMP25k/DNA complexes treated by nuclease. It can be seen that naked DNA is degraded by nuclease, so its electrophoresis band disappears (lane 7), and the electrophoresis results of various vector/DNA complexes are consistent with group I. Based on the fact that no significant DNA was reflected in the holes of lanes 8 and 9, it was hypothesized that the protective ability of PEI was weaker than that of the vector. Lanes 14–18 show the electrophoresis results of PEI10k/DNA, PEI25k/DNA, RMP10k/DNA, RMP25k/DNA and FA-RMP25k/DNA complexes treated with Active Ingredient sodium, indicating that Active Ingredient sodium can release DNA from the complex through competitive binding. Lanes 20–24 show that Active Ingredient sodium could release DNA from the vector/DNA complexes treated with nuclease, which fully proves that the DNA in these complexes could resist degradation by nuclease. The electrophoresis results in group V further verified this conclusion, because the complexes in lanes 26–30 were first treated with Active Ingredient sodium, and then treated with nuclease. The results showed that the DNA was prematurely replaced by sodium Active Ingredient and completely degraded by nuclease, so no electrophoretic bands were shown.

3.5. Cytotoxicity evaluation

The cytotoxicity of RMPs, RMPs/DNA, FA-RMP25k and FA-RMP25k/DNA complexes was evaluated in 293T, HeLa, AML-12 and HepG2 cells by MTT assay. Fig. 4a, c, e and g demonstrates that the cytotoxicity of these polymers is dependent on the concentration. In 293T cells, RMP10k is safer than PEI10k at the same concentration, and RMP25k and FA-RMP25k show similar cytotoxicity, which is lower than that of PEI25k. Fig. 4a shows that in 293T cells, the cell survival rates

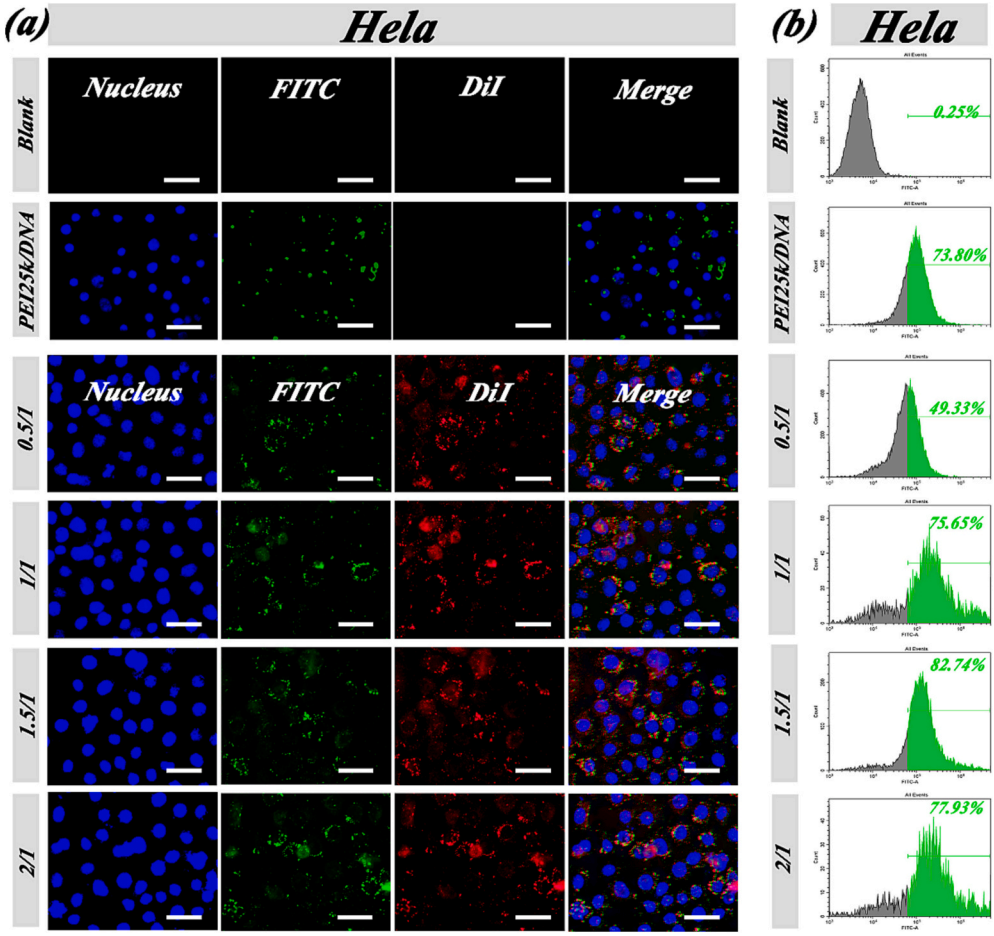

Fig. 6. Cell uptake results of RMP25k/DNA complexes in HeLa cells. (a) Fluorescence images (400×) of HeLa cells treated by DiI-FITC-RMP25k/DNA complexes (scale bar = 50 μm). (b) FCM results of the uptake efficiency of DiI-FITC-RMP25k/DNA complexes.

treated with RMP25k and FA-RMP25k at concentrations of 25 μg/mL were 83.47 % and 81.21 %, respectively, whereas the cell survival rate treated with PEI25k was 53.85 %. Fig. 4c shows that in HeLa cells, the survival rates of cells that were treated with RMP10k, RMP25k and FA-RMP25k with a concentration of 25 μg/mL were 87.8 %, 86.7 % and 80.4 %, respectively, while the cell survival rates of PEI10k and PEI25k were 70.9 % and 57.7 %, respectively. Interestingly, the results in Fig. 4e–g can be seen in AML-12 and HepG2 cells exhibiting a similar trend to the 293T and Hela cytotoxicity results, in which RMP10k, RMP25k, and FA-RMP25k exhibited higher cellular activity than the corresponding molecular weight PEIs. These results suggest that the cytotoxicity of PEI can be effectively reduced by cell membrane grafting. As seen in Fig. 4b, d, f and h, the cytotoxicity of RMP10k/DNA, RMP25k/DNA and FA-RMP25k/DNA complexes showed a concentration-dependent manner; however, the relative viability of 293T and HeLa cells exceeded 80 %, except at a mass ratio of 5/1.

In conclusion, RMPs and FA-RMP25k possess a higher safety profile than PEI10k and PEI25k.

3.6. *In vitro cell uptake*

High cell uptake efficiency is one of the core characteristics of gene delivery vectors. In this work, the uptake efficiency of complexes with different mass ratios in 293T and HeLa cells was studied.

The uptake results of the complexes in 293T cells are presented in Supporting Information, and the fluorescence microscope observation results showed they were successfully ingested by 293T cells (Figs. S2a and S3a). As shown in Figs. S2a, S3a, and S4a, the red fluorescence (DiI labeled membrane in RMPs and FA-RMP25k) and green fluorescence (FITC labeled PEI in RMPs and FA-RMP25k) completely overlap, with most of them scattered around the blue light spot (DAPI labeled nucleus) and some overlapping. This intuitively demonstrates that RMPs/DNA and FA-RMP25k/DNA complexes can be effectively absorbed by cells. This conclusion can also be more clearly verified by the results of the CLSM shown in Fig. S4c. The results from FCM analysis demonstrated that 293T cells had significantly higher uptake efficiency for RMP10k/DNA (Fig. S2b) and RMP25k/DNA (Fig. S3b) complexes with the same mass ratio than PEI/DNA. Additionally, when RMP25k was modified with FA molecules, the cell uptake was further increased (Fig. S4b). The highest efficiency of uptake for the RMP10k/DNA, RMP25k/DNA, and FA-RMP25k/DNA complexes was 64.49 %, 73.42 %, and 88.36 %, respectively, when the mass ratios were 3/1, 1.5/1, and 2/1.

The FCM results in HeLa cells revealed that RMP10k/DNA (Fig. 5b), RMP25k/DNA (Fig. 6b), and FA-RMP25k/DNA (Fig. 7b) had a higher uptake efficiency compared to PEI/DNA. Interestingly, the uptake efficiency of RMP10k/DNA and RMP25k/DNA was lower in HeLa cells than in 293T cells, however, the uptake efficiency of FA-RMP25k/DNA in HeLa cells was higher, reaching a maximum of 96.08 % at a mass ratio of 2:1 (Fig. 7b). This suggests that FA-RMP25k/DNA has tumor cell targeting capabilities. To sum up, the RMPs complexes prepared in this study had a higher uptake efficiency than PEI in both cell types, and the FA modification gave the complexes tumor cell targeting properties, resulting in a higher uptake efficiency in tumor cells.

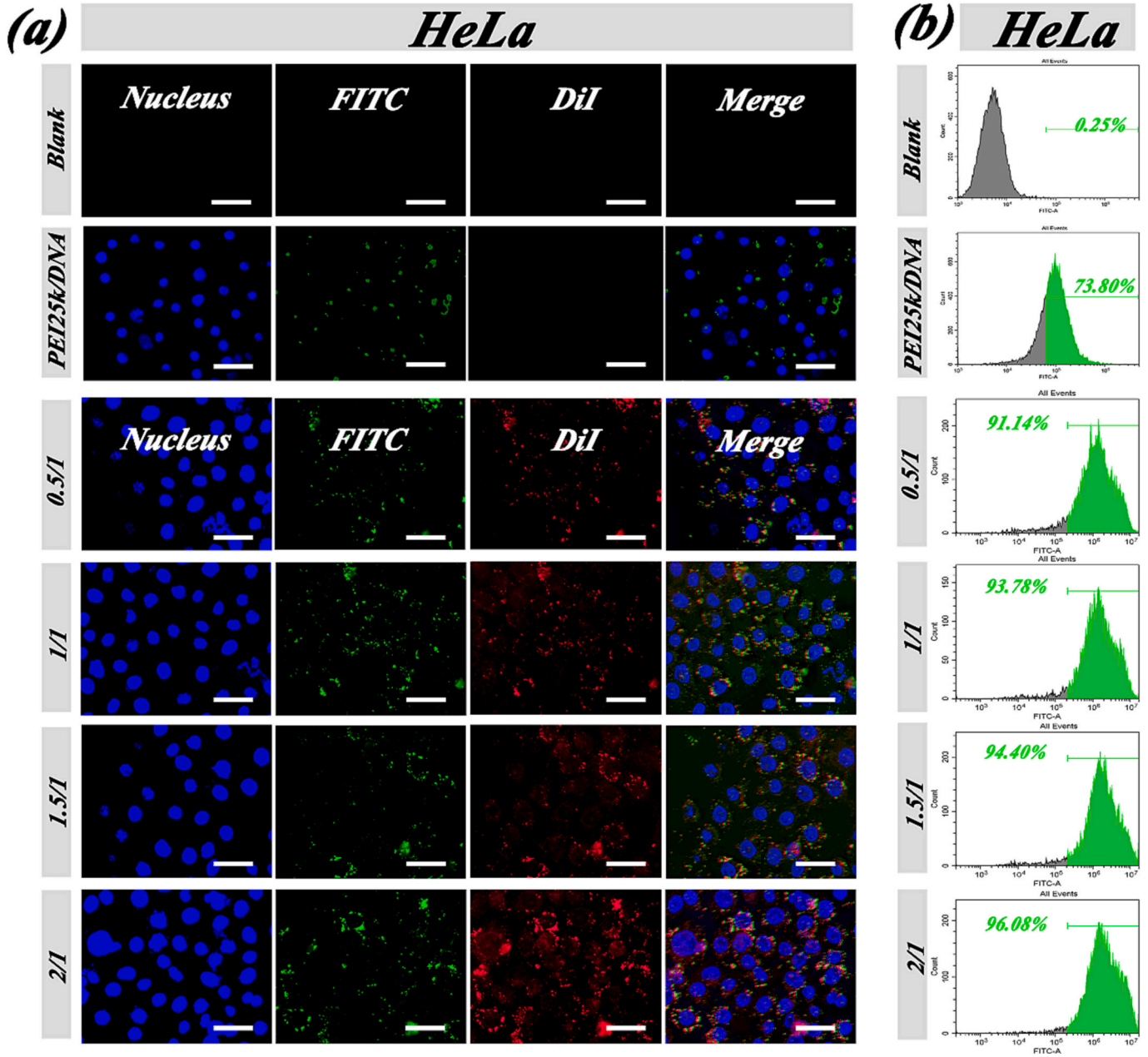

Fig. 7. Cell uptake results of FA-RMP25k/DNA complexes in HeLa cells. (a) Fluorescence images (400×) of HeLa cells treated by DiI-FITC-FA-RMP25k/DNA complexes. Scale bar = 50 μm. (b) FCM results of the uptake efficiency of DiI-FITC-FA-RMP25k/DNA complexes.

3.7. *In vitro* gene transfection

The EGFP plasmid was used as the reporter gene to assess the transfection efficiency of each polymer *in vitro*. As seen in Figs. 8, 9 and 10, GFP expression was successfully observed in both cell lines treated with different polymers. Different mass ratios resulted in varying transfection efficiencies. In 293T cells, the highest transfection efficiency was observed with RMP10k/DNA at mass ratios of 2/1 and 3/1, exceeding 46 % (Fig. 8b and f). RMP25k/DNA achieved the greatest efficiency of 69.93 % at a mass ratio of 3/1 (Fig. 8d and h), which was higher than those of PEI10k/DNA (Fig. 8a) and PEI25k/DNA (Fig. 8c), yet still lower than the commercial reagents (Fig. 8e). In HeLa cells, the transfection efficiency of the complexes was lower than in 293T cells. RMP10k and RMP25k (Fig. 9b, d, f, and h) demonstrated the highest transfection efficiency at a mass ratio of 3/1, reaching 10.55 % and 20.13 %, respectively, which was lower than the commercial reagents (Fig. 9e).

It is interesting to observe that the transfection efficiency of the FA-RMP25k/DNA complex in 293T cells is slightly higher than that of the RMP25k/DNA complex (Fig. 10a and c). However, in HeLa cells, the transfection efficiency of the FA-RMP25k/DNA complex is about 15 % higher than that of the RMP25k/DNA complex (Fig. 10b and e). This is attributed to the overexpression of the FA receptor in tumor cells, which enables the FA-RMP25k/DNA complex to have a higher cellular uptake efficiency in tumor cells than in normal cells. Additionally, the responsiveness of the disulfide bond in FA-RMP25k to GSH promotes the release of DNA in the complex and consequently enhances the transfection efficiency of the complex in HeLa cells. This is further corroborated by the average fluorescence intensity trends of 293T and HeLa cells transfected with the complex (Figs. 8g, i, 9g, i, 10d and f).

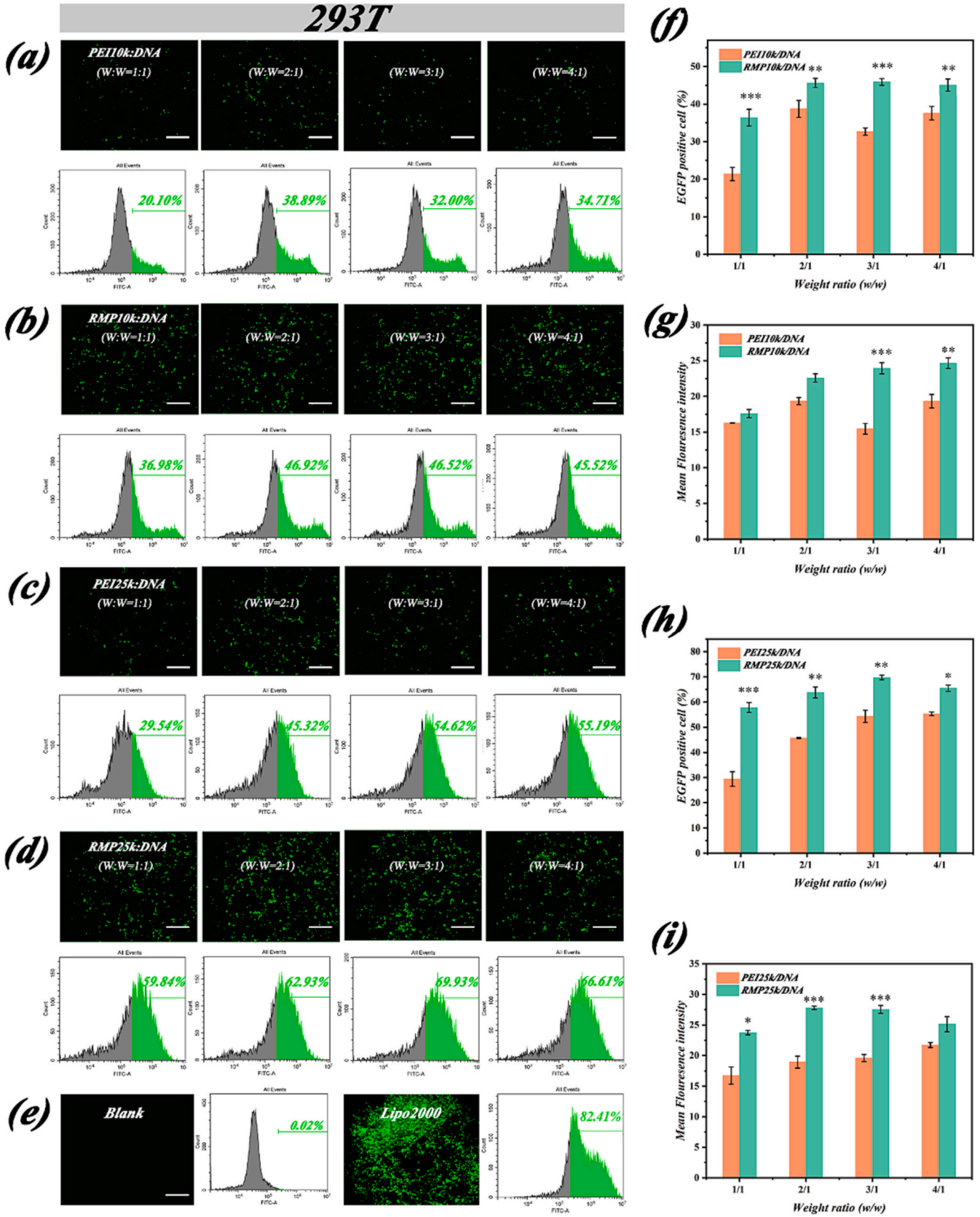

Fig. 8. Transfection results of RMPs/DNA complexes in 293T cells. Transfection results of (a) PEI10k/DNA, (b) RMP10k/DNA, (c) PEI25k/DNA and (d) RMP25k/DNA complexes. (e) Transfection results of blank and Lipo2000. (f) Histogram of transfection of PEI10k/DNA and RMP10k/DNA. (g) Histogram of transfection efficiency and mean fluorescence intensity of PEI10k/DNA and RMP10k/DNA complexes. Histogram of transfection efficiency (h) and mean fluorescence intensity (i) of PEI25k/DNA and RMP25k/DNA. Scale bar = 1000 μm. (The experimental group was compared with the PEI/DNA group, mean ± SD, n = 3; $*p \leq 0.05$, $**p \leq 0.01$, $***p \leq 0.005$.)

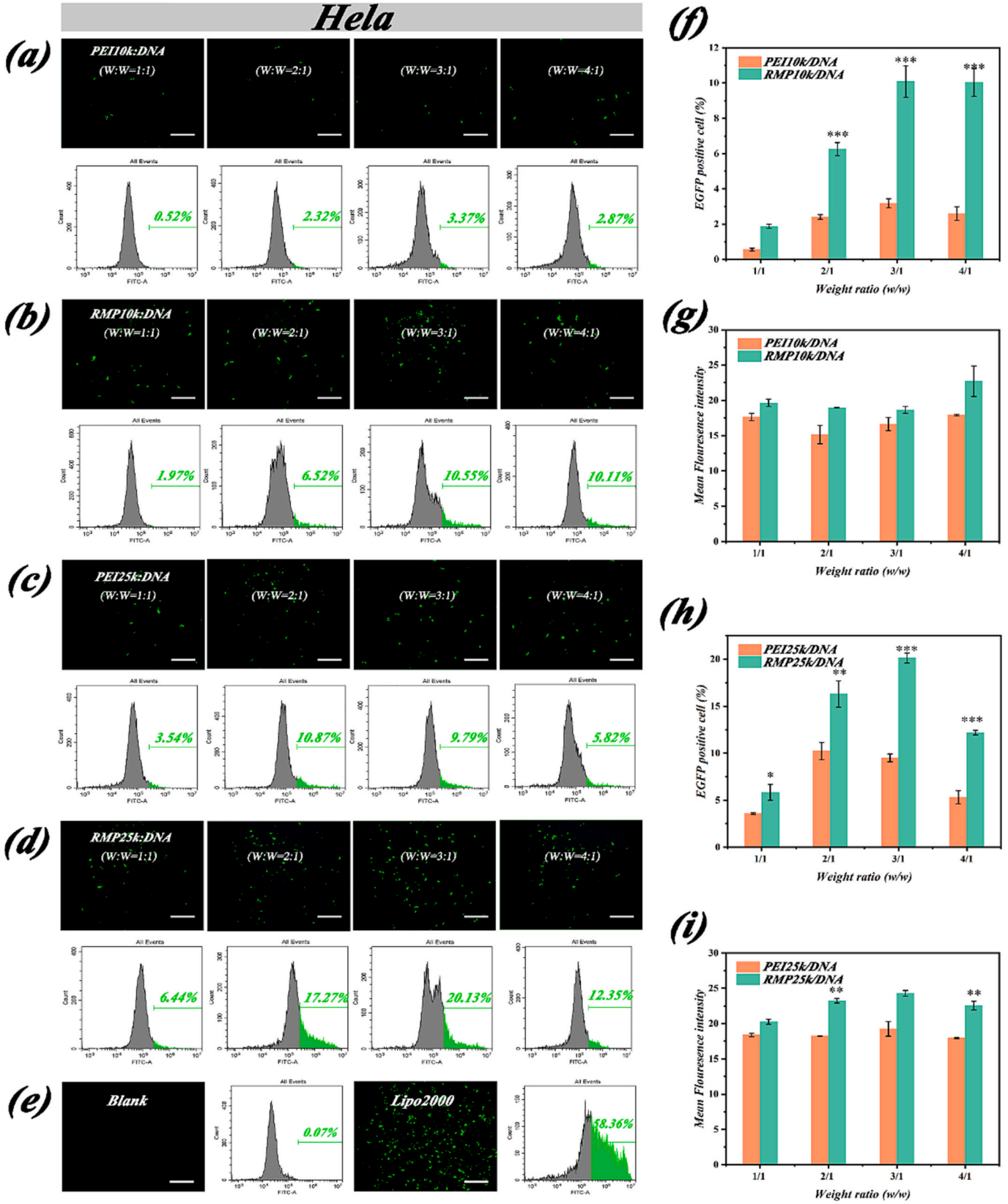

Fig. 9. Transfection results of RMPs/DNA complexes in HeLa cells. Transfection results of (a) PEI10k/DNA, (b) RMP10k/DNA, (c) PEI25k/DNA and (d) RMP25k/DNA complexes. (e) Transfection results of blank and Lipo2000. (f) Histogram of transfection of PEI10k/DNA and RMP10k/DNA. (g) Histogram of transfection efficiency and mean fluorescence intensity of PEI10k/DNA and RMP10k/DNA complexes. Histogram of transfection efficiency (h) and mean fluorescence intensity (i) of PEI25k/DNA and RMP25k/DNA. Scale bar = 1000 μm. (The experimental group was compared with the PEI/DNA group, mean ± SD, n = 3; $*p \leq 0.05$, $**p \leq 0.01$, $***p \leq 0.005$.)

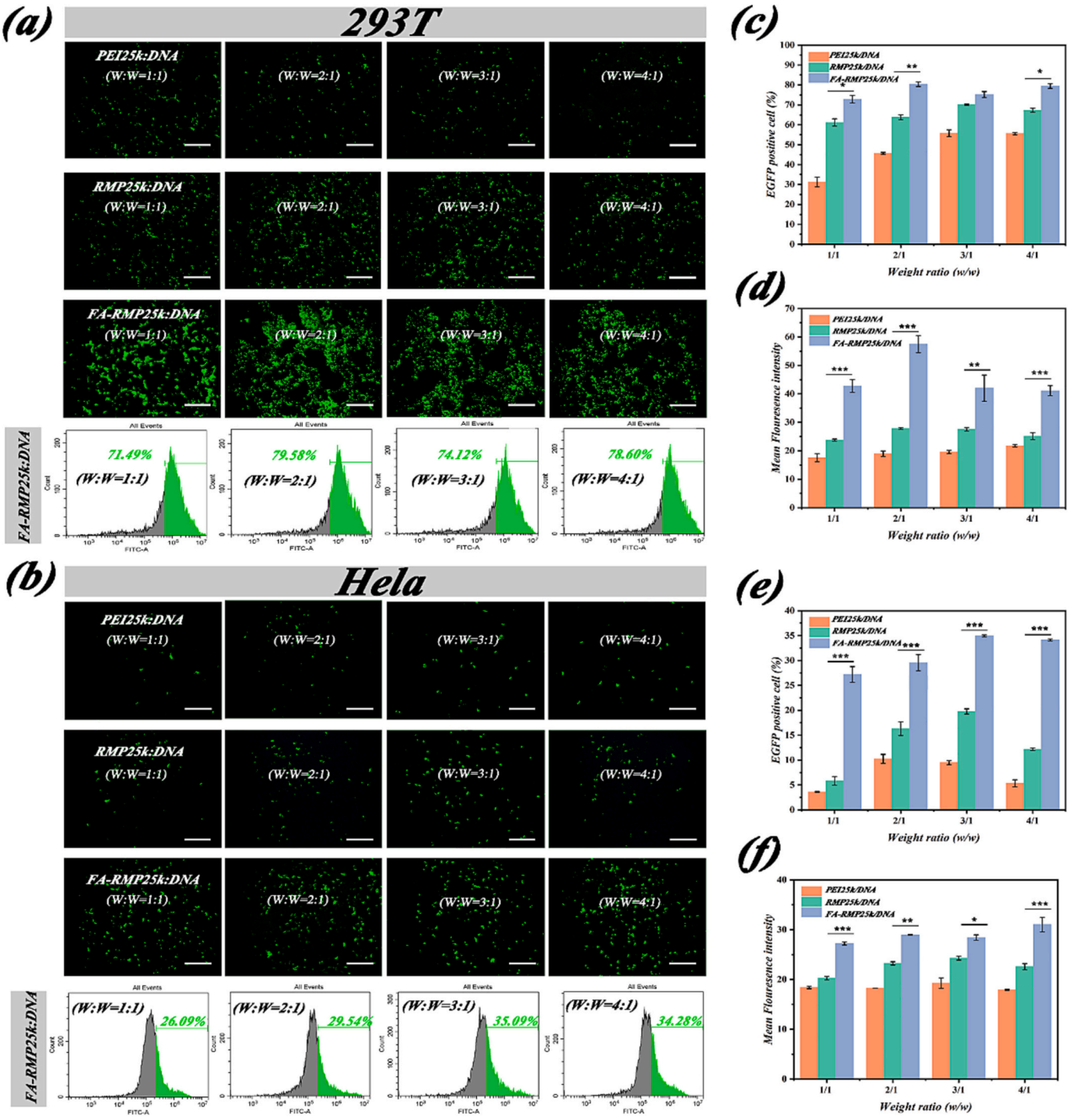

Fig. 10. Transfection results of FA-RMP25k/DNA complexes. (a) Transfection results in 293T cells. (b) Transfection results in HeLa cells. Histogram of (c) transfection efficiency and (d) mean fluorescence intensity in 293T cells. Histogram of transfection efficiency (e) and mean fluorescence intensity (f) in HeLa cells. Scale bar = 1000 μm. (The FA-RMP25k/DNA group was compared to the RMP25k/DNA group, mean ± SD, n = 3; $*p \leq 0.05$, $**p \leq 0.01$, $***p \leq 0.005$.)

4. Conclusion

In this work, a novel biocompatible polymer, FA-RMP25k, was designed and synthesized for the preparation of safe and efficient gene delivery vectors. The biocompatible erythrocyte membrane was successfully cross-linked with PEI through disulfide bonding, which not only achieved the responsive release of DNA in the tumor microenvironment but also significantly reduced the cytotoxicity of PEI. RMPs/DNA complexes have excellent stability, DNA binding capacity and responsive release efficiency. The results of *in vitro* transfection experiments with EGFP in 293T and HeLa cells showed a significant increase in the transfection efficiency of RMPs/DNA complexes compared to PEI/DNA complexes. Transfection result of FA-RMP25k/DNA complex from HeLa cells showed that successful modification of the targeting molecule FA significantly improved the transfection ability of PEI25k/DNA complex in cancer cells. In sum, this work constructed a tumor-targeted gene nano delivery system that can be used as a safe and effective gene vector for gene therapy.

CRediT authorship contribution statement

Haoxiang Huang: Conceptualization, Methodology, Project administration, Resources, Supervision, Writing – review & editing. **Yanlin Sun:** Formal analysis, Investigation, Methodology. **Mingjie Wang:** Formal analysis, Methodology, Validation. **Zhaojun Yang:** Investigation, Methodology. **Yong Shi:** Investigation, Methodology. **Liang Liu:** Funding acquisition, Resources, Supervision.

Declaration of competing interest

The authors declare that they have no known competing financial interests or personal relationships that could have appeared to influence the work reported in this paper.

Acknowledgments

This work was financially supported by the National Natural Science Foundation of China (21602166), Natural Science Foundation of Hubei Province (2020CFB760) and Research and Innovation Initiatives of WHPU (2021Y11).

Appendix A. Supplementary data

Supplementary data to this article can be found online at https://doi.org/10.1016/j.ijbiomac.2023.128354.

References

[1] P. Seth, Vector-mediated cancer gene therapy - an overview, Cancer Biol. Ther. 4 (5) (2005) 512–517.
[2] C. Zhang, Q.-T. Wang, H. Liu, Z.-Z. Zhang, W.-L. Huang, Advancement and prospects of tumor gene therapy, Chin. J. Cancer 30 (3) (2011) 182–188.
[3] M. Tristan-Manzano, P. Justicia-Lirio, N. Maldonado-Perez, M. Cortijo-Gutierrez, K. Benabdellah, F. Martin, Externally-controlled systems for immunotherapy: from bench to bedside, Front. Immunol. 11 (2020).
[4] A. Paul, R. Anand, S.P. Karmakar, S. Rawat, N. Bairagi, S. Chatterjee, Exploring gene knockout strategies to identify potential drug targets using genome-scale metabolic models, Sci. Rep. 11 (1) (2021).
[5] J.Q. Tan, W. Yu, CRISPR as a tool in tumor therapy: a short review, Biotechnol. Appl. Biochem. 67 (6) (2020) 875–879.
[6] C.M. Chen, Z.J. Yang, X.J. Tang, Chemical modifications of nucleic acid drugs and their delivery systems for gene-based therapy, Med. Res. Rev. 38 (3) (2018) 829–869.
[7] R.J. Chandler, C.P. Venditti, Gene therapy for metabolic diseases, Transl. Sci. Rare Dis. 1 (1) (2016) 73–89.
[8] H. Hosseinkhani, W.J. He, C.H. Chiang, P.D. Hong, D.S. Yu, A.J. Domb, K.L. Ou, Biodegradable nanoparticles for gene therapy technology, J. Nanopart. Res. 15 (7) (2013).
[9] S.-B. Yong, J.Y. Chung, Y. Song, Y.-H. Kim, Recent challenges and advances in genetically-engineered cell therapy, J. Pharm. Investig. 48 (2) (2018) 199–208.
[10] H. Zu, D.C. Gao, Non-viral vectors in gene therapy: recent development, challenges, and prospects, AAPS J. 23 (4) (2021).
[11] U. Bezeljak, Cancer gene therapy goes viral: viral vector platforms come of age, Radiol. Oncol. 56 (1) (2022) 1–13.
[12] B. Caffery, J.S. Lee, A.A. Alexander-Bryant, Vectors for glioblastoma gene therapy: viral & non-viral delivery strategies, Nanomaterials 9 (1) (2019).
[13] Y.K. Sung, S.W. Kim, Recent advances in the development of gene delivery systems, Biomater. Res. 23 (1) (2019).
[14] H. Yin, R.L. Kanasty, A.A. Eltoukhy, A.J. Vegas, J.R. Dorkin, D.G. Anderson, Non-viral vectors for gene-based therapy, Nat. Rev. Genet. 15 (8) (2014) 541–555.
[15] W.T. Godbey, K.K. Wu, A.G. Mikos, Poly(ethylenimine) and its role in gene delivery, J. Control. Release 60 (2–3) (1999) 149–160.
[16] S. Taranejoo, J. Liu, P. Verma, K. Hourigan, A review of the developments of characteristics of PEI derivatives for gene delivery applications, J. Appl. Polym. Sci. 132 (25) (2015).
[17] Z.Z. Xu, G.B. Shen, X.Y. Xia, X.Y. Zhao, P. Zhang, H.H. Wu, Q.F. Guo, Z.Y. Qian, Y. Q. Wei, S.F. Liang, Comparisons of three polyethyleneimine-derived nanoparticles as a gene therapy delivery system for renal cell carcinoma, J. Transl. Med. 9 (2011).
[18] X.X. Tian, A.H. Shi, J.Z. Wu, Construction of biomimetic-responsive nanocarriers and their applications in tumor targeting, Anti Cancer Agents Med. Chem. 22 (12) (2022) 2255–2273.
[19] L. Liu, Z.J. Yang, C.B. Liu, M.Y. Wang, X. Chen, Preparation of PEI-modified nanoparticles by Active Ingredient self-polymerization for efficient DNA delivery, Biotechnol. Appl. Biochem. 70 (2) (2023) 824–834.
[20] S. Siegman, N.F. Truong, T. Segura, Encapsulation of PEGylated low-molecular-weight PEI polyplexes in hyaluronic acid hydrogels reduces aggregation, Acta Biomater. 28 (2015) 45–54.
[21] L. Liu, C.B. Liu, Z.J. Yang, Y.R. Chen, S.H. Wu, X. Chen, Safe and efficient DNA delivery based on tannic acid-ion coordination encapsulation, Soft Mater. 21 (1) (2023) 37–52.
[22] X. Li, Y.J. Chen, M.Q. Wang, Y.J. Ma, W.L. Xia, H.C. Gu, A mesoporous silica nanoparticle - PEI - fusogenic peptide system for siRNA delivery in cancer therapy, Biomaterials 34 (4) (2013) 1391–1401.
[23] Q.Y. Yu, Y.R. Zhan, J. Zhang, C.R. Luan, B. Wang, X.Q. Yu, Aromatic modification of low molecular weight PEI for enhanced gene delivery, Polymers 9 (8) (2017).
[24] A. Malek, F. Czubayk, A. Aigner, PEG grafting of polyethylenimine (PEI) exerts different effects on DNA transfection and siRNA-induced gene targeting efficacy, J. Drug Target. 16 (2) (2008) 124–139.
[25] L. Liu, Y.J. Yan, D.N. Ni, S.H. Wu, Y.R. Chen, X. Chen, X.M. Xiong, G. Liu, TAT-functionalized PEI-grafting rice bran polysaccharides for safe and efficient gene delivery, Int. J. Biol. Macromol. 146 (2020) 1076–1086.
[26] Z.H. Guo, Y.J. Li, Y.G. Fu, T.Q. Guo, X. Li, S. Yang, J. Xie, Enhanced antisense oligonucleotide delivery using cationic liposomes incorporating fatty acid-modified polyethylenimine, Curr. Pharm. Biotechnol. 15 (9) (2014) 800–805.
[27] M. Zhang, C. Lou, A. Cao, Progresses on active targeting liposome drug delivery systems for tumor therapy, Sheng wu yi xue gong cheng xue za zhi = Journal of biomedical engineering = Shengwu yixue gongchengxue zazhi 39 (3) (2022) 633–638.
[28] A. Poddar, J.J. Conesa, K. Liang, S. Dhakal, P. Reineck, G. Bryant, E. Pereiro, R. Ricco, H. Amenitsch, C. Doonan, X. Mulet, C.M. Doherty, P. Falcaro, R. Shukla, Encapsulation, visualization and expression of genes with biomimetically mineralized zeolitic imidazolate framework-8 (ZIF-8), Small 15 (36) (2019).
[29] N.S. Templeton, D.D. Lasic, New directions in liposome gene delivery, Mol. Biotechnol. 11 (2) (1999) 175–180.
[30] X.F. Hao, Q. Li, H.N. Wang, K. Muhammad, J.T. Guo, X.K. Ren, C.C. Shi, S.H. Xia, W.C. Zhang, Y.K. Feng, Red-blood-cell-mimetic gene delivery systems for long circulation and high transfection efficiency in ECs, J. Mater. Chem. B 6 (37) (2018) 5975–5985.
[31] H. Liu, Y.Y. Su, X.C. Jiang, J.Q. Gao, Cell membrane-coated nanoparticles: a novel multifunctional biomimetic drug delivery system, Drug Deliv. Transl. Res. 13 (3) (2023) 716–737.
[32] S. Han, Y. Lee, M. Lee, Biomimetic cell membrane-coated DNA nanoparticles for gene delivery to glioblastoma, J. Control. Release 338 (2021) 22–32.
[33] Z. Fang, M. Zhang, R. Kang, M.X. Cui, M.D. Song, K.H. Liu, A cancer cell membrane coated nanoparticles-based gene delivery system for enhancing cancer therapy, Int. J. Pharm. 629 (2022).
[34] Q. Xia, Y.T. Zhang, Z. Li, X.F. Hou, N.P. Feng, Red blood cell membrane-camouflaged nanoparticles: a novel drug delivery system for antitumor application, Acta Pharm. Sin. B 9 (4) (2019) 675–689.
[35] N. Rani, Z.M. Alzubaidi, H. Azhari, F. Mustapa, M. Amin, Novel engineering: biomimicking erythrocyte as a revolutionary platform for drugs and vaccines delivery, Eur. J. Pharmacol. 900 (2021).
[36] E. Mirhadi, M. Mashreghi, M.F. Maleki, S.H. Alavizadeh, L. Arabi, A. Badiee, M. R. Jaafari, Redox-sensitive nanoscale drug delivery systems for cancer treatment, Int. J. Pharm. 589 (2020).
[37] P. Mi, Stimuli-responsive nanocarriers for drug delivery, tumor imaging, therapy and theranostics, Theranostics 10 (10) (2020) 4557–4588.
[38] C.L. Zhu, X.W. Wang, Z.Z. Lin, Z.H. Xie, X.R. Wang, Cell microenvironment stimuli-responsive controlled-release delivery systems based on mesoporous silica nanoparticles, J. Food Drug Anal. 22 (1) (2014) 18–28.
[39] H.Q. Dong, M. Tang, Y. Li, Y.Y. Li, D. Qian, D.L. Shi, Disulfide-bridged cleavable PEGylation in polymeric nanomedicine for controlled therapeutic delivery, Nanomedicine 10 (12) (2015) 1941–1958.
[40] K. Yan, Y.C. Feng, K. Gao, X.J. Shi, X.B. Zhao, Fabrication of hyaluronic acid-based micelles with glutathione-responsiveness for targeted anticancer drug delivery, J. Colloid Interface Sci. 606 (2022) 1586–1596.
[41] G. Zuber, C.D. Muller, J.P. Behr, Targeted gene delivery to cancer cells with nanometric DNA particles enveloped with folic acid using a polymerisable anchor, Technol. Cancer Res. Treat. 4 (6) (2005) 637–643.
[42] T.Y. Xiao, X.Y. Cao, X.Y. Shi, Dendrimer-entrapped gold nanoparticles modified with folic acid for targeted gene delivery applications, J. Control. Release 172 (1) (2013) E114–E115.
[43] X.F. Cong, J. Chen, R. Xu, Recent progress in bio-responsive drug delivery systems for tumor therapy, Front. Bioeng. Biotechnol. 10 (2022).
[44] B. Hasan-Nasab, P. Ebrahimnejad, P. Ebrahimi, F. Sharifi, M. Salili, F. Shahlaee, A. Nokhodchi, A promising targeting system to enrich Active Ingredient antitumor efficacy: folic acid targeted nanoparticles, J. Drug Deliv. Sci. Technol. 63 (2021).
[45] J.H. Jeong, S.H. Kim, S.W. Kim, T.G. Park, In vivo tumor targeting of ODN-PEG-folic acid/PEI polyelectrolyte complex micelles, J. Biomater. Sci. Polym. Ed. 16 (11) (2005) 1409–1419.
[46] P. Chanphai, H.A. Tajmir-Riahi, DNA binding efficacy with functionalized folic acid-PAMAM nanoparticles, Chem. Biol. Interact. 290 (2018) 52–56.
[47] X.L. Zhao, Z.Y. Li, H.B. Pan, W.G. Liu, M.M. Lv, F. Leung, W.W. Lu, Enhanced gene delivery by chitosan-disulfide-conjugated LMW-PEI for facilitating osteogenic differentiation, Acta Biomater. 9 (5) (2013) 6694–6703.
[48] E. Assadpour, S.M. Jafari, Y. Maghsoudlou, Evaluation of folic acid release from spray dried powder particles of pectin-whey protein nano-capsules, Int. J. Biol. Macromol. 95 (2017) 238–247.

[49] X.X. Sun, N. Wang, L.Y. Yang, X.K. Ouyang, F.F. Huang, Folic acid and PEI modified mesoporous silica for targeted delivery of curcumin, Pharmaceutics 11 (9) (2019).
[50] X.J. Zhang, Y. Chen, Y. Chen, An AFM-based pit-measuring method for indirect measurements of cell-surface membrane vesicles, Biochem. Biophys. Res. Commun. 446 (1) (2014) 375–379.
[51] A. Taniguchi, T. Akita, K. Yasuda, Y. Miyazaki, Analysis of degradation in PEMFC caused by cell reversal during air starvation, Int. J. Hydrog. Energy 33 (9) (2008) 2323–2329.